Fish and Shellfish Immunology 88 (2019) 244–253

Contents lists available at ScienceDirect

Fish and Shellfish Immunology

journal homepage: www.elsevier.com/locate/fsi

Full length article

# Elucidation of mechanism for host response to VHSV infection at varying temperatures *in vitro* and *in vivo* through proteomic analysis

Se-Young Cho[a,1], Rachael A. Protzman[a,b,1], Yeong O. Kim[b,1], Bipin Vaidya[b], Myung-Joo Oh[c], Joseph Kwon[a,**], Duwoon Kim[b,*]

[a] Biological Disaster Analysis Group, Korea Basic Science Institute, Daejeon, 34133, Republic of Korea
[b] Department of Food Science and Technology and Foodborne Virus Research Center, Chonnam National University, Gwangju, 61186, Republic of Korea
[c] Department of Aqualife Medicine, College of Fisheries and Ocean Science, Chonnam National University, Yeosu, 59626, Republic of Korea

ARTICLE INFO

*Keywords:*
Viral hemorrhagic septicemia virus (VHSV)
Rearing temperature
FHM cell
Zebrafish (*Danio rerio*)
Proteomic analysis
GLI2

ABSTRACT

Seasonal temperature has a major influence on the infectivity of pathogens and the host immune system. Viral hemorrhagic septicemia virus (VHSV) is one such pathogen that only causes the mortality of fish at low temperatures. This study aims to discover the host defense mechanism and pathway for resistance to VHSV at higher temperatures. We first observed the VHSV infection patterns at low and higher temperatures in fathead minnow (FHM) cells (20 °C and 28 °C) and zebrafish (15 °C and 25 °C). In comparison to the 20 °C infection, FHM cells infected at 28 °C showed decreased apoptosis, increased cell viability, and reduced VHSV N gene expression. In zebrafish, infection at 25 °C caused no mortality and significantly reduced the N gene copy number in comparison to infection at 15 °C. To explore the antiviral infection mechanisms induced by high temperature *in vitro* and *in vivo*, the changes in the proteomic profile were measured through UPLC-$MS^E$ analysis. ACADL, PTPN6, TLR1, F7, A2M, and GLI2 were selected as high temperature-specific biomarkers in the FHM cell proteome; and MYH9, HPX, ANTXR1, APOA1, HBZ, and MYH7 were selected in zebrafish. Increased immune response, anticoagulation effects, and the formation of lymphocytes from hematopoietic stem cells were analyzed as functions that were commonly induced by high temperature *in vitro* and *in vivo*. Among these biomarkers, GLI2 was predicted as an upstream regulator. When treated with GANT58, a GLI-specific inhibitor, cell viability was further reduced due to GLI2 inhibition during VHSV infection at varying temperatures in FHM cells, and the mortality in zebrafish was induced earlier at the low temperature. Overall, this study discovered a new mechanism for VHSV infection *in vitro* and *in vivo* that is regulated by GLI2 protein.

## 1. Introduction

Environmental change modulates patterns of host susceptibility and/or pathogen virulence, revealing the context-dependent nature of disease epidemiology [1]. For instance, temperature has been documented as a critical environmental feature modulating host-pathogen interaction outcomes [2]. Temperature is particularly notable for being causally linked to the annual winter occurrence of the influenza virus [3]. It has been shown that $CD8^+$ T cell activation and differentiation are increased with increasing body temperature [4], allowing for improved immune response at higher temperatures. However, at lower temperatures, MAVS antiviral signaling protein is attenuated, reducing the induction of IFNs and IFN-stimulated genes and preventing adequate immune response [5].

One pathway that has been implicated in regulating immune response is the Hedgehog (Hh) signaling pathway. Activation of the Hh pathway is known to help maintain homeostasis in adult tissue by modulating tissue repair [6]. During infection by a pathogen, Hh signaling has been shown to both positively and negatively regulate T cell proliferation and cytokine expression [7]. Specifically, previous studies have reported the role of GLI family zinc finger 2 (GLI2), an Hh transcriptional activator, in immune dysregulation and fibrosis induction due to HIV and hepatitis C viral replication, respectively [8]. Another study found that when GLI2 was activated in T-cells, it caused the downregulation of heat shock proteins [9], which are often expressed in response to environmental stress, such as cold stress [10].

* Corresponding author.
** Corresponding author.
*E-mail addresses:* joseph@kbsi.re.kr (J. Kwon), dwkim@jnu.ac.kr (D. Kim).
[1] These authors contributed equally to this work.

https://doi.org/10.1016/j.fsi.2019.02.037
Received 24 August 2018; Received in revised form 31 January 2019; Accepted 18 February 2019
Available online 22 February 2019
1050-4648/ 

Viral hemorrhagic septicemia virus (VHSV) is a negative-stranded *Novirhabdovirus* that shows high mortality at low temperatures and has been isolated from 70 species of finfish worldwide [11]. A long term (1982–2014) observation of seasonal variations in water temperature showed a high fluctuation in water temperature in the Yellow and East China Seas, with an overall cooling effect since the late 1990s [12]. As VHSV occurs frequently during fluctuations in water temperature [13], these seasonal variations are a cause for concern. VHSV infection causes enlarged internal organs and hemorrhaging of the skin, muscle, kidney, and liver, resulting in high mortality rates in economically valuable fish, threatening the aquaculture industry [14]. Similar to other Rhabdoviruses, the rearing temperature affects VHSV replication and the severity of infection [15–18]. The optimal temperature for VHSV replication is 14–15 °C, but the virus has been shown to replicate at as low as 4 °C *in vitro* [19,20]. Likewise, *in vivo* mortality and viral replication in VHSV-infected fish increase as the rearing temperatures reduce [13, 21−22]. Isshiki et al. (2001) have reported mortality due to VHSV infection in olive flounder at 8–15 °C [23]. In contrast, viral pathogenicity and replication are greatly diminished at temperatures ≥ 20 °C [13,22].

The effect of low temperature on VHSV has been shown in several models such as fathead minnow (FHM) cells, rainbow trout, and olive flounder [24–26]. FHM cells have been shown to be susceptible to VHSV replication at 15 °C, but the overexpression of a lectin originating from rock bream was able to block the replication at the same temperature [27]. The survival mechanisms observed in fish reared at higher temperatures could result from enhanced adaptive immunity, such as T lymphocyte responses, or diminished viral resilience [18]. Alternatively, temperature-associated survival has been suggested to result from regulation of Mx and interferon expression by the innate immune response [21]. Proteomic analyses have also been performed to study responses to VHSV infection on the *in vitro* level in FHM cells, and on the *in vivo* level in zebrafish fins [27–29]. However, conclusive evidence on the mechanisms controlling the reduction of VHSV infection severity by increasing the temperature remains limited.

In the current study, we explored the effect of rearing temperature variation on host pathogenic response by measuring changes to the proteome of VHSV-infected FHM cells and zebrafish. One of the major regulating proteins was found to be GLI2. By inhibiting its expression in FHM cells and zebrafish, we further discovered the role of GLI2 in regulating VHSV infection during exposure to different temperatures.

## 2. Materials and methods

### 2.1. Cells and zebrafish

Fathead minnow (FHM) cells were grown at 20 °C in L-15$_{10}$ medium, consisting of Leibovitz's L-15 (Welgene, Gyeongsang, South Korea) supplemented with 10% fetal bovine serum (FBS), 100 U/mL penicillin and 100 μg/mL streptomycin (Gibco, Grand Island, NY, USA). Zebrafish weighing around 300 mg (wet basis) were raised in 28 °C circulating water according to the zebrafish manual (zfin.org) in a Zebrafish Auto System (Genomic Design Co., Ltd., Daejeon, South Korea) before beginning the experiment. They were kept at a 14:10 h day/night cycle and fed twice a day with Tetra Bits Complete fish food.

### 2.2. Virus preparation

VHSV genogroup IVa stock ($10^{8.8}$ TCID$_{50}$/mL) was obtained from the lab of Professor Myung-Joo Oh of the Chonnam National University Department of Aqualife Medicine (Yeosu, South Korea). FHM cells were infected with VHSV (MOI = 0.1) in L-15$_{10}$ medium diluted 1:4 in L-15 medium and incubated at 20 °C until significant cytopathic effect (CPE) was observed. Then the stock was collected and subjected to three freeze-thaw cycles before centrifugation and collection of supernatant. The virus ($10^{8.3-8.8}$ TCID$_{50}$/mL) was stored at −80 °C in 1 mL aliquots before experimental infection.

### 2.3. Cell viability

FHM cells cultured for 24 h were infected with VHSV (MOI = 0.1) and incubated at 20 and 28 °C for 48 h. Cell viability was evaluated with cell counting kit-8 (CCK-8, Dojindo Laboratories, Kumamoto, Japan) following the manufacturer's protocol. First, FHM cells were plated in 96-well plates (SPL Life Science, Seoul, Korea) at a density of $1.0 \times 10^5$ cells/well in L-15$_{10}$ medium, and incubated at 20 °C for 24 h. For GANT58 treatment, the culture medium was changed with 100 μL of L-15$_{10}$ containing GANT58 (100 μM, Santa Cruz Biotech., Dallas, TX, USA). The treated cells were incubated at 20, 24, and 28 °C for 24 h. Subsequently, the medium was changed with 100 mL of fresh medium containing VHSV (MOI = 0.2) and incubated again at the same temperatures for 41 h. After incubation, CCK-8 assay was performed and analyzed according to the manufacturer's instructions.

### 2.4. Zebrafish challenge test

VHSV challenge was performed using zebrafish adapted to 15 °C water in a temperature-controlled room or 15 °C water bath for 3 days before 2 h immersion infection with VHSV ($10^{5.8-6.3}$ TCID$_{50}$/mL). Fifteen zebrafish were randomly selected for each test group, including non-treated groups of 15 °C uninfected (15NM), 15 °C VHSV-infected (15NV), 25 °C uninfected (25NM), and 25 °C VHSV-infected (25NV). After a 3-day temperature adjustment, immersion infection was performed [26] by diluting VHSV stock $10^2$ to $10^3$ times in zebrafish system water. The fish were transferred to new system water after infection, and the mortality was monitored daily for 3 weeks. Three fish from each group were randomly sampled at 3 dpi. No food was given to the fish during the infection, and half of the water in each fish tank was replaced every two days to prevent hypoxic conditions. For GANT58 treatment, 25 mM of GANT58 was diluted to 100 mg/kg of fish body weight in phosphate buffered saline (PBS) and orally administered to zebrafish in 6 μL doses by combining methods from Dang et al. [30] and Kulkarni et al. [31]. The fish were anesthetized in MS-222 (Sigma-Aldrich, St. Louis, MO, USA), held vertically with a moist sponge, and GANT58 was slowly released from the pipette in 10-s intervals. The micropipette was aimed directly into the stomach past the level of the gills in order to prevent leaking from the gills or regurgitation.

### 2.5. Apoptosis assay

Cell apoptosis was analyzed using the Muse™ Cell Analyzer (Merck Millipore, Billerica, MA, USA) according to the manufacturer's protocol. FHM cells were incubated at 20 °C for 24 h, and then inoculated with VHSV at 20 and 28 °C for 48 h. The cells were harvested using trypsin-EDTA and stained with Annexin V and Dead Cell Reagent (7-aminoactinomycin D, 7-AAD; Merck Millipore, Billerica, MA, USA). After staining, the cells were incubated in the dark for 20 min and the events for dead, late apoptosis, early apoptosis, and live cells were counted using the Muse Cell Analyzer.

### 2.6. Real time PCR and TCID$_{50}$ assay

Total RNA was isolated from healthy and VHSV-infected and/or GANT58-treated zebrafish and FHM cells using RNAiso Plus reagent (Takara Bio, Shiga, Japan) according to the manufacturer's instructions. Aliquots of RNA were reverse transcribed into cDNA using 1 μL 6mer random primer, 2 μL dNTP, 0.5 μL recombinant RNase inhibitor (Takara Bio), and 1 μL MMLV RT, 4 μL 5X MMLV RT buffer, and 2 μL 5X DTT (Beams Biotechnology, Seongnam, Korea). Quantitative RT-PCR was performed using the SYBR Green Master Kit (Takara Bio) in a Thermal Cycler Dice Real Time System (Takara Bio). The conditions for the absolute quantification of the VHSV N gene were as follows: initial

denaturation at 95 °C for 30 s followed by 40 cycles of denaturation at 95 °C for 5 s and 60 °C for 30 s, and 1 cycle of dissociation at 95 °C for 15 s, 60 °C for 30 s, and 95 °C for 15 s. For relative quantification of primers, the following conditions were used: initial denaturation at 95 °C for 30 s, 45 cycles of denaturation at 95 °C for 5 s, 55 °C for 10 s, and 72 °C for 20 s, and 1 cycle of dissociation similar to absolute quantification. Viral titers of VHSV-infected samples at different temperatures (20 and 28 °C for FHM cells, and 15 and 25 °C for zebrafish) were determined by the $TCID_{50}$ method [32]. All primer and standard sequences can be found in Supplementary Table S1.

### 2.7. Immunofluorescence assay

FHM cells were seeded on glass coverslips that had been placed in 24-well plates until 80% confluence. Cells were infected with VHSV (MOI = 0.2) and fixed with cold 4% paraformaldehyde at 42 h post-infection (hpi) and then rinsed with PBS. The cells were permeabilized by incubating the slides with 0.1% Triton X-100 in PBS for 10 min at room temperature. The cells were treated with blocking buffer (PBS with 2% bovine serum albumin) for 1 h, and primary antibody (Anti-VHSV G protein monoclonal antibody, clone 23H21, Creative Diagnostics, working dilution 1:200) was added to the cells for 2 h in a humidified chamber at room temperature. Following rinsing with PBS, slides were incubated with anti-rabbit secondary antibody with fluorescent probe (FITC-coupled anti-rabbit IgG, H&L, Abcam, Cambridge, MA, USA) for 1 h at room temperature. Cell nuclei were counterstained with 0.1% DAPI (Invitrogen). The fluorescent images were examined using a confocal laser scanning microscope (TCS SP5/AOBS/Tandem, Leica, Jena, Germany) and analyzed with Leica LAS AF lite software (Ver. 2.3.5).

### 2.8. Cytosol protein extract and tube-gel digestion

Cells and frozen whole zebrafish were rinsed twice with ice-cold PBS. Zebrafish were homogenized in, and cells were re-suspended in, a protease inhibitor cocktail (Thermo Scientific, Rockford, IL, USA) and centrifuged for 30 min at 16,000 × *g* at 4 °C. Sample supernatants were collected and incubated for 5 min on ice, then centrifuged at 12,000 × *g* at 4 °C for 15 min. Proteins in the supernatant were quantified using a Detergent Compatible (DC) Protein Assay Kit (Bio-Rad, Hercules, CA, USA) and then 100 μg of each sample was lyophilized in a Speed Vac. Proteins were digested using the "Tube-Gel" digestion protocol of Han et al. [33]. First, the cytosolic protein pellet was re-suspended in 50 μL of 6 M urea, 5 mM EDTA, and 2% (w/v) SDS in 0.1 M triethylammonium bicarbonate (TEABC) and incubated at 37 °C to dissolve for 30 min. The proteins were then reduced by the addition of 10 μL of 20 mM Tris (2-carboxyethyl) phosphine and alkylated by adding 20 μL of 20 mM iodoacetamide at room temperature for 30 min in the dark. The tube-gel was prepared by adding 18.5 μL of 40% (v/v) acrylamide/bisacrylamide (29:1), 2.5 μL of 10% (w/v) ammonium persulphate, and 1 μL of 100% tetramethylethylenediamine directly to the protein solution. The gel was then cut into small pieces and rinsed three times with 1 mL of 50% (v/v) acetonitrile (ACN) in TEABC. The dehydrated gel samples were then digested with 15 μL trypsin (protein: trypsin, 10:1, w/w) in 25 mM TEABC and incubated overnight at 37 °C. The digested peptides were vacuum extracted twice with a solution of 50 mM ammonium bicarbonate in 50% ACN and 5% trifluoroactic acid (TFA). The resultant peptide extracts were collected, lyophilized, and dissolved in 0.5% TFA prior to Nano UPLC-$HDMS^E$ analysis.

### 2.9. Nano UPLC-$HDMS^E$ analysis

Digested peptides were analyzed using a nano-ACQUITY Ultra Performance Liquid Chromatograph™ (UPLC) equipped with a Synapt G2-Si High Definition Mass Spectrometer (HDMS, Waters Corp., Milford, MA, USA), which was operated in a data-independent manner coupled with ion mobility [34]. The MS was operated in positive electrospray ionization (ESI) resolution mode with a limit resolution of > 250,000 full width at half maximum. During data acquisition, MS and MS/MS were set at low (4 eV) and elevated (14–40 eV) collision energies, respectively, on the transfer collision cell with a scan time of 0.5 s per function over 100–2500 *m/z*. MS and MS/MS spectra data were collected in triplicate. Tryptic peptides (1.5 mg) were loaded onto the enrichment column with mobile phase A, containing 3% acetonitrile (ACN) and 0.1% formic acid in water, and mobile phase B, containing 97% ACN and 0.1% formic acid in water. A stepwise gradient was applied at a flow rate of 250–300 nL/min, made up of 40% mobile phase B for 95 min, 40–70% mobile phase B for 20 min, and 80% mobile phase B for 10 min. Sodium formate (1 μM/min) was used to calibrate the time-of-flight analyzer in the range of *m/z* 100–2500, and [Glu1]-fibrinopeptide (*m/z* 785.8426) at 2 μL/min was used for lock mass correction.

### 2.10. Protein identification and relative quantification

Proteins were identified and quantified using Progenesis QI for Proteomics (QIP) version 1.0 (Nonlinear Dynamics, Newcastle, UK) [35]. NCBI FHM genome database (Genome ID: 13167) was used to identify FHM cell proteins, and the UniProtKB/Swiss-Prot proteome database for *Danio rerio* (Accessed: 7/11/2017) was used to identify zebrafish proteins. The whole protein and amino acid database for FHM cells was built with BLASTX on the basis of the fathead minnow (*Pimephales promelas)* whole genome sequence from NCBI (https://www.ncbi.nlm.nih.gov/nuccore/JNCE00000000).

### 2.11. Bioinformatics analysis

The up- and down-regulated proteins in sample sets were collectively used for biological function and network analysis. Only proteins containing at least one unique peptide (not assigned to other proteins) were considered as validly identified. Ingenuity Pathway Analysis (IPA, Qiagen, version 44691306, http://www.ingenuity.com) was used to identify biological function, pathway and networks of related proteins derived from IPA Knowledge Base. The Knowledge Base is a large structured library assembled from scientific literature database-supported relationships between molecules, biological functions, and diseases derived from numerous experimental systems in mice, rats, and humans. IPA can automatically recognize potentially connected interactions from its own database with uploaded gene IDs. The FHM database was matched against the human genome in a BLAST search in order to upload FHM cell proteins. The zebrafish Uniprot accession numbers could automatically convert into human homologues, which were then used to observe relationships between regulated proteins.

### 2.12. Statistical analysis

All experimental samples were analyzed in triplicate, and statistical analysis was performed using Prism ver. 5.0 (GraphPad, LaJolla, CA, USA). Results were expressed as mean standard deviation with significance represented as $p \leq 0.05$ (*), $p \leq 0.01$ (**), or $p \leq 0.001$ (***). Where appropriate, one-way or two-way ANOVA were used with post hoc analysis performed by Tukey's test or Bonferroni's test, respectively.

## 3. Results and discussion

### 3.1. Temperature dependency of VHSV infection in vitro and in vivo

To determine the effect of temperature on VHSV infection, cell viability and apoptosis were first measured in FHM cells in four samples including uninfected at 28 °C (28M), uninfected at 20 °C (20M), VHSV-infected at 28 °C (28 V), and VHSV-infected at 20 °C (20 V). The VHSV titer ($TCID_{50}$) and N gene expression were also measured to indicate the

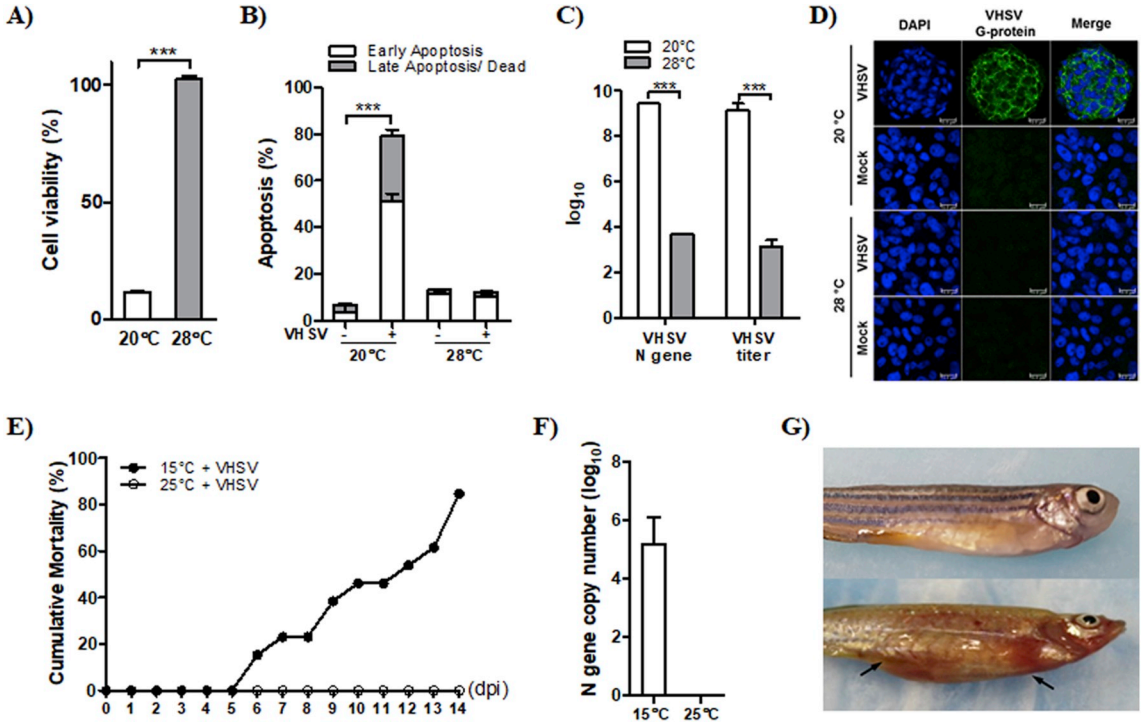


**Fig. 1. VHSV infectivity according to cell culture temperature and rearing temperature in FHM cells and zebrafish.**
(A) Cell viability of infected FHM cells measured at 20 °C and 28 °C using CCK-8 reagent. (B) Percent apoptosis comparing VHSV infection with non-infection, measured using the Muse™ Cell Analyzer. (C) Comparative analysis of viral infectivity at 20 °C and 28 °C by measuring the VHSV N gene by qPCR and the titer by the $TCID_{50}$ method. (D) Immunofluorescence imaging of FHM cells infected by VHSV at 20 °C and 28 °C by measuring VHSV G protein with DAPI as a cell marker. (E) Cumulative mortality of infected zebrafish at 15 °C and 25 °C. (F) VHSV N gene copy number measured by qPCR analysis in infected zebrafish at 3 dpi. (G) Visible comparison of external symptoms observed in normal fish (upper) and VHSV-infected fish (lower). Error bars represent the mean ± SD (n = 3). ***$p \leq 0.001$ (Bonferroni post-test). VHSV = Viral hemorrhagic septicemia virus. Scale bar = 15.0 μm.

infectivity of the virus and the viral copy number, respectively [36]. The results revealed that the lower temperature caused a cell viability of only 11.9% (Fig. 1A), which was comparable to the reports of other studies on VHSV infection in walleye cells *in vitro* and bluegill fish *in vivo* that showed that lowering the temperature reduced cell viability and increased mortality, respectively [13,20]. Total apoptosis (early and late) decreased with increasing temperature in VHSV-infected cells (Fig. 1B), dropping from 79.0% at 20 °C down to 12.5% at 28 °C. More importantly, the total apoptosis of VHSV-infected cells at 28 °C was not significantly different from uninfected cells, indicating that VHSV infection inhibited viral replication at higher temperature. Evidence for this was provided by VHSV N-gene copy number measurements and VHSV G-protein expression using immunofluorescence. At 48 hpi, the VHSV N-gene copy number was measured to be 9.4 log at 20 °C and 3.7 log at 28 °C, respectively (Fig. 1C). Similar results were obtained when measuring the titer using the $TCID_{50}$ method ($10^{9.1}$ $TCID_{50}$/mL at 20 °C and $10^{3.1}$ $TCID_{50}$/mL at 28 °C). The Rhabdovirus glycoprotein (G) is required for the efficient viral assembly and budding before virion release from the host cell [37]. In order to visualize this process in VHSV, immunofluorescence assay of the G protein was performed (Fig. 1D). As shown, the VHSV G protein was only detected in 20 °C virus-infected cells. It is suspected that the viral copy number was too low to be detected in the 28 °C virus-infected cells due to low infection at 48 hpi. It has been reported that in the host, apoptotic response was blocked during early VHSV infection in olive flounder at 15 °C to allow for viral replication, but that the apoptosis system had remained effective during early infection at the higher temperature of 20 °C [43]. In this study, we considered that the operation of the apoptosis system at higher temperature had already efficiently blocked VHSV replication during the early infection stage, preventing the need for further apoptosis.

The zebrafish was chosen as the *in vivo* model for this study as it has already been established as an animal model for VHSV infection [39]. We first performed a VHSV infection challenge test on the zebrafish in order to determine if the rearing temperature had an effect on viral infectivity. The groups were separated by virus and temperature similarly to the FHM cells at the low temperature of 15 °C and the higher temperature of 25 °C (15M, 15 V, 25M, and 25 V). In Fig. 1E (mock groups not shown), the first observed mortality occurred at 6 days post infection (dpi) in the 15 V group, and the mortality rate steadily increased until reaching a cumulative mortality of 84.6% at 14 dpi. There was no mortality observed in the 25 °C VHSV-infected group. It has been reported that inflammation and necrosis could already be observed at 72 hpi in VHSV-infected olive flounder, and that the VHSV N gene copy number rose significantly [38]. When we also measured the VHSV N gene in whole zebrafish at 3 dpi, we found the copy number to be 5.7 log at 15 °C (Fig. 1F). Shortly before death, the virus-infected zebrafish at 15 °C showed abnormal swimming patterns and swam closer to the surface of the water. As shown in Fig. 1G, mortality symptoms frequently included hemorrhaging at the head, mouth, and gills, and intestinal swelling at the base of the abdomen, all consistent with previous reports [14,40]. Until the end of the experiment, there were no mortality, viral replication, or external clinical signs observed in the fish infected at 25 °C. This is similar to other *in vivo* studies that reported no mortality in olive flounder at the higher temperatures of 17 or 20 °C [26,41].

Our observations are consistent with other studies that showed a reduction in the pathogenicity of VHSV or the resistance to viral infection at higher temperatures [24]. There have been studies on the antiviral immune-related genes that respond to VHSV infection at low temperatures [42], as well as the host immune response at low and higher temperatures in olive flounder [43]. There have even been tests studying VHSV infectivity at low temperatures through proteomic and transcriptomic analyses in zebrafish, rainbow trout, and olive flounder [29]. One recent study sequenced the transcriptome of VHSV-infected

olive flounder at cold and warm temperatures, but did not interpret the host defense network [44]. Until now, the reason for antiviral resistance to VHSV at high temperatures has not been discovered. Therefore, in order to discover the mechanism for host resistance to VHSV at high temperatures *in vitro* and *in vivo*, we compared the low and higher temperature proteomes from infected FHM cells (20 °C and 28 °C) and zebrafish (15 °C and 25 °C), and elucidated the protein network pathways and biological functions.

### 3.2. Proteomic changes and biological functions

In order to examine the proteomic changes to the cell and whole organism infected by VHSV, relative quantitative proteomic analysis was performed. There were 247 proteins identified in the fish cells, which were categorized by temperature and infection as 20 °C uninfected/mock (20M), 20 °C virus-infected (20 V), 28 °C uninfected (28M), and 28 °C virus-infected (28 V). For the zebrafish, there were 103 proteins identified in the groups 15 °C uninfected (15M), 15 °C virus-infected (15 V), 25 °C uninfected (25M), and 25 °C virus-infected (25 V) (Supplementary Table S2). Hierarchical clustering was then performed using the proteomics data in order to find correlations between each group. Similar to Fig. 1D, which revealed that only the 20 V group showed the phenotype for VHSV in FHM cells, 20 V was also the only distinguished group in the clustering analysis (tree scale value 0.123), with the higher temperature virus-infected group being recognized as similar to the mock. For zebrafish, proteins were classified into 2 distinct groups, virus-infected and uninfected, with a tree scale value of 0.157. It was also confirmed that the virus-infected group was further classified according to the change in temperature with a tree scale value of 0.049 (Supplementary Figs. S1A and S1B). This shows that there was a difference between mock and virus infection, but that the influence of temperature was only present during the virus infection. The only group commonly distinguished in both models was the low temperature virus-infected group. To examine the clustering information in more detail, bioinformatics analysis was performed for each group.

In order to study the biological functions, the 75 FHM cell and 50 zebrafish genes with high similarity to human genes were uploaded into IPA, and the biological information was subsequently investigated. As shown in Table 1, there were 15 diseases and biofunctions, including body temperature, that were annotated as major functions in FHM cells. The IPA knowledge database predicted that in the 20 V group, which shows the phenotype for VHSV infection, the inflammatory response became inactivated (z-score: −0.685). There were 13 functions annotated to be main functions in the zebrafish proteome, including morbidity and mortality, and it was predicted that in the low temperature (15 V) condition, morbidity and mortality were inactivated (z-score: −1.733) and phagocytosis was activated (z-score: 1.452) (Table 2). The inactivation of mortality-related signals in the low temperature VHSV-infected zebrafish group was considered to be a signal for trying to overcome the infection, especially in the infection stage at 3 dpi. We suspect that one of the causes of mortality was that phagocytosis did not stay activated at later stages of infection in the low temperature condition. Phagocytes are required for the removal of apoptotic cells, which is an important process in removing the virus from the body [45]. According to a study by Avunje et al., VHSV infection in olive flounder was able to override the host apoptosis system to allow for viral replication and delayed apoptotic response at the lower infection temperature of 15 °C [43]. This was shown by the initial rise in granzyme expression that decreased during the peak of viral replication and increased again in the later infection stage. In the same study, caspase 3 was more highly expressed at the higher temperature of 20 °C in the early stage of infection, which may have been enough to suppress viral replication, and could be the reason for the high cell viability and absence of zebrafish mortality at higher temperatures in the current study.

Next, the biological functions of FHM cells and zebrafish were further explored by category. In FHM cells, hematological system development was the most highly represented with 14%, followed by inflammatory response (7%), and immune cell trafficking (5%) (Supplementary Fig. S2A and Table 1). The most highly represented categories in zebrafish were organismal injury and abnormalities (11%), hematological system development (9%), and inflammatory response (7%) (Supplementary Fig. S2B and Table 2). Hematological system development and inflammatory response were represented in both FHM cells and zebrafish. These results are reflective of previous literature, which show VHSV infection to cause extensive damage to hematopoietic tissues, such as inflammation and necrosis in the kidney and spleens [19,39]. Hematopoietic stem cells are important for their differentiation into T and B lymphocytes, which are responsible for adaptive immunity, and myeloid cells such as granulocytes, macrophages, dendritic cells, and mast cells, which are required during both innate and adaptive immunity [46]. Studies have also shown the role of inflammatory response in VHSV infection, such as the increase in proinflammatory IL-1β during early infection, and TNFα in later infection to attenuate IL-1β expression [25]. Histopathology of the heart of infected olive flounder also found the epicardium of the ventricle penetrated by inflammatory cells [23].

### 3.3. High temperature and virus-dependent expressed proteins

Next, in order to distinguish between high temperature-dependent proteins (Type A) and high temperature-dependent virus resistance

**Table 1**
Diseases and functions from IPA analysis significantly affected by VHSV infection in FHM cells.

| Annotation of Diseases or Functions | *p*-Value* | Molecules |
|---|---|---|
| Cell division of macrophages | 6.6.E−03 | A2M |
| Differentiation of Th1-like cells | 3.3.E−03 | GLI2 |
| Differentiation of Th2-like cells | 1.0.E−02 | GLI2 |
| Antagonization of T lymphocytes | 3.3.E−03 | PTPN6 |
| Activation of B-2 lymphocytes | 1.3.E−02 | PTPN6 |
| Binding of antigen presenting cells | 4.5.E−03 | A2M, SERPINE1, PTPN6 |
| Generation of B-2 lymphocytes | 6.6.E−03 | PTPN6 |
| Movement of monocyte-derived macrophages | 3.9.E−03 | SERPINE1, PTPN6 |
| Initiation of coagulation of blood | 1.3.E−02 | F7. |
| Activation of innate immune system | 1.0.E−02 | TLR1 |
| Inflammatory response | 1.5.E−02 | TUBA1A, NLRC3, TLR1, F7, PTPN6, CASR, SERPINE1, LRRK2, COL18A1 |
| Body temperature | 6.7.E−04 | ACADL, NLRC3, SERPINE1, CAMKK2 |
| Nighttime core body temperature | 2.0.E−02 | ACADL |
| Intracranial hemorrhage | 2.4.E−03 | GABRA4, F7, SERPINE1, COL18A1 |
| Edema | 5.9.E−03 | GABRA4, F7, GLI2, SERPINE1, COL18A1, MYOM1 |

*The p-value was calculated using Fisher's Exact Test by Ingenuity Pathway Analysis (IPA).

**Table 2**
Diseases and functions from IPA analysis significantly affected by VHSV infection in zebrafish.

| Annotation of Diseases or Functions | *p*-Value* | Molecules |
|---|---|---|
| Cell death of gonadal cell lines | 1.E−02 | ANTXR1, APOA1 |
| Cell polarity formation of T lymphocytes | 1.E−02 | MYH9. |
| Deformation of red blood cells | 2.E−05 | HBZ, HBE1 |
| Differentiation of TH17 lineage cells | 2.E−03 | HPX |
| Diffuse B-cell lymphoma | 1.E−02 | TUBA1A, MYO5C, ANTXR1, MYOM2, MYO5B, NAV3 |
| Diffuse large B-cell lymphoma | 7.E−03 | TUBA1A, MYO5C, ANTXR1, MYOM2 |
| Inflammation of organ | 1.E−02 | KRT8, TUBA1A, CKM, APOA1, ALDOA, GAPDH, HPX, CKB, NAV3, MYH9 |
| Morbidity or mortality | 3.E−03 | SCRIB, KRT8, MYH7, ATP2A1, LMO7, PDE4DIP, ALDOA, PLA2G6, CKB, ANK3, MYH9, HBZ, ACTG1, ANTXR1, MYH11, APOA1, ACTA1 |
| Phagocytosis | 3.E−03 | MYO5A, APOA1, PLA2G6, CKB, MYH9 |
| Platelet clot | 2.E−02 | MYH9 |
| Quantity of B-lymphocyte derived cell lines | 1.E−02 | MYH7. |
| Recruitment of inflammatory monocytes | 1.E−02 | APOA1 |
| Thrombosis of blood | 1.E−02 | ANTXR1 |

*The p-value was calculated using Fisher's Exact Test by Ingenuity Pathway Analysis (IPA).

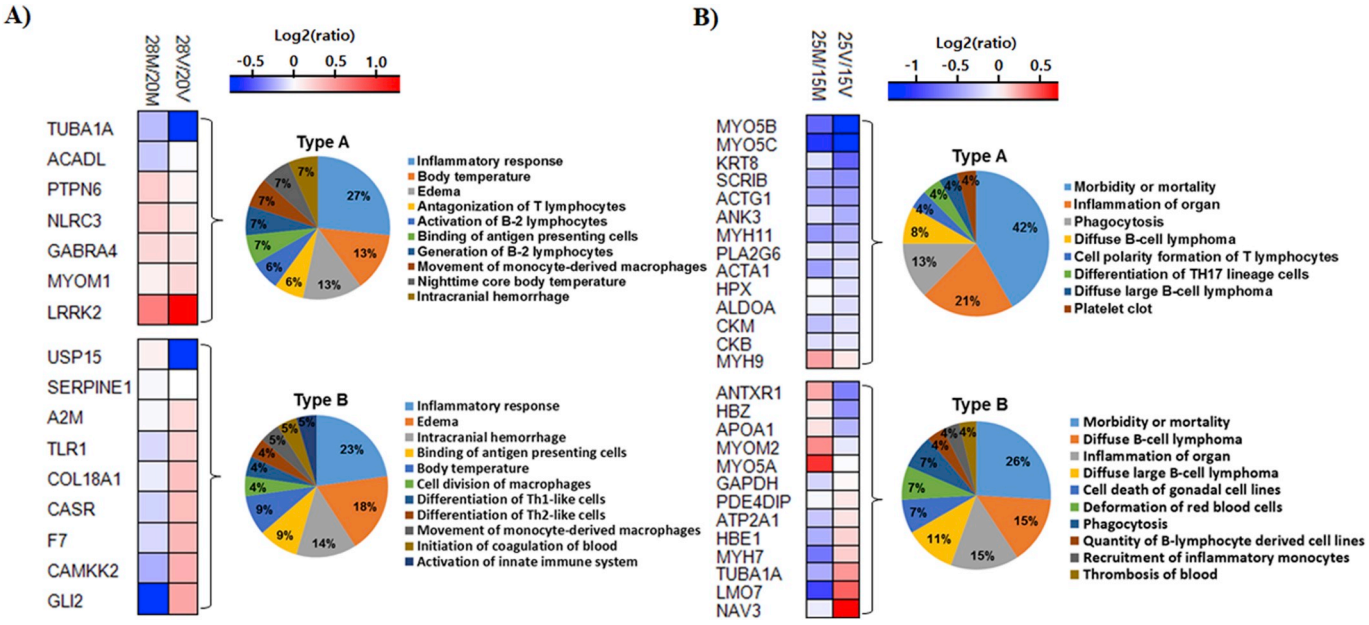


**Fig. 2. Characterization of proteomics-identified proteins based on expression patterns in (A) FHM cells and (B) zebrafish.**
Proteins were categorized into Type A (High Temperature-Dependent Proteins) based on the same expression pattern between mock and virus infection conditions when the ratios of higher temperature (28 °C in FHM cells and 25 °C in zebrafish) to low temperature (20 °C in FHM cells and 15 °C in zebrafish) were compared. Type B (High temperature-dependent Viral Resistance Proteins) proteins were categorized based on opposing expression patterns between mock and virus infection conditions when comparing the ratio of higher temperature to low temperature.

proteins (Type B) in FHM cells, the expression patterns of 28M/20M and 28 V/20 V ratios were observed (Fig. 2A). Proteins upregulated by the higher temperature were marked in red and downregulated proteins were marked in blue. Type A proteins were categorized by keeping the same expression pattern for both the presence and absence of VHSV infection, and were considered to be temperature-dependent regardless of virus exposure. Type B proteins had opposite expression patterns between the infected and uninfected groups, and were considered to be resistant to virus infection at the higher temperature. The FHM cell proteins that were related to inflammatory response, body temperature, edema, intracranial hemorrhage, binding of antigen presenting cells, and movement of monocyte-derived macrophages were evenly distributed between Type A and Type B groups. Functions unique to the Type A group were nighttime core body temperature, production and activity of B-2 lymphocytes, and antagonization of T lymphocytes. The proteins related to these functions were ACADL and PTPN6. These showed significant differences in expression between high temperature and low temperature, and when infected by VHSV, they were able to maintain their unique expression patterns, which is necessary for viral resistance at high temperatures. The functions that were only found in the Type B group were activation of the innate immune system, initiation of the coagulation of blood, differentiation of Th1- and Th2-like cells, and cell division of macrophages (Fig. 2A). The proteins related to these functions were TLR1, F7, A2M, and GLI2. The expressions of these proteins at high temperature were significantly different at low temperature, and they seemed to change expression for the sake of survival during the virus infection, contributing to their antiviral activity at high temperatures. In particular, these proteins showed anticoagulation-related functions. The activation of the coagulation system in 20 V indicated the excessive coagulation of blood during VHSV infection, which could be a primary cause of mortality in VHSV-infected fish at relatively low temperature. One study on the transcriptomic profile of trout showed both upregulated and downregulated coagulation-related genes in VHSV-infected turbot, suggesting that self-regulation of coagulation is necessary for host survival, similarly to how both pro- and anti-inflammatory molecules are necessary for survival [47]. Another study in FHM cells showed that VHSV infection caused a deficiency in F2 protein, favoring anticoagulation and leading to hemorrhaging [27].

Antoniak et al. also reported that the activation of coagulation during a virus infection is a protective mechanism to limit the spread of the infection; however, excessive clotting can lead to intravascular coagulation and subsequent hemorrhaging during hemorrhagic viral infections, including Ebola and Dengue hemorrhagic fever [48]. It is possible that the coagulation of blood is activated in response to VHSV infection similarly to the infection of other viruses, such as HIV, herpes, dengue, and Ebola virus infections, resulting in the mortality of VHSV-infected fish [48–52]. The increased expression of F7 in the 28 V sample compared to 20 V could protect the cell from excessive coagulation. Correspondingly, the optimum temperature for the coagulating activity of F7 was reported to be 15 °C, which gradually decreases with increasing temperature [53].

In zebrafish, the proteins related to the functions of morbidity or mortality, inflammation of organ, phagocytosis, and diffuse large B-cell and B-cell lymphoma were evenly distributed between Type A and B groups. Functions only found in the Type A group were cell polarity formation of T lymphocytes, differentiation of TH17 lineage cells, and platelet clotting (Fig. 2B). Proteins related to these functions were MYH9 and HPX. These proteins only showed significant changes in expression due to change in temperature that were maintained regardless of virus infection, allowing them to resist against virus infection at high temperatures. Functions only expressed in the Type B group were cell death of gonadal cell lines, deformation of red blood cells, quantity of B-lymphocyte derived cell lines, recruitment of inflammatory monocytes, and thrombosis of blood (Fig. 2B). The proteins related to these functions were ANTXR1, APOA1, HBZ, HBE1, and MYH7. Through the proteomic analysis of FHM cells and zebrafish, it could be confirmed that the antiviral effects at high temperature overall resulted from the significant changes in functions such as the differentiation and maturation of hematopoietic stem cells into lymphocytes during the production of blood, as well as immune response and anticoagulation effects.

### 3.4. Combined network of high temperature- and virus-dependent biomarkers

The interactions of proteins related to unique functions in Type A and B groups were identified through IPA network analysis. The network in Fig. 3 was created by combining biomarkers that contribute to mortality or cell death during virus infection at the low temperature condition from FHM cells and zebrafish. In the FHM cells, it was confirmed that GLI2 was the main protein linked to survival as it formed connections with anticoagulant proteins and lymphocyte-activating phosphatase. All of the proteins involved in these networks were downregulated due to VHSV infection at low temperature. The major biomarkers in zebrafish were shown to be involved with the mortality and inflammation of organ networks. It was identified by the IPA knowledge database that MYOD1 was an upstream regulator of these biomarkers (Supplementary Fig. S3), and IPA further marked GLI2 as upstream to MYOD1 as confirmed by previous reports [54,55].

Research on the effects of GLI2 on immune response are conflicting. It has been shown that GLI2 negatively regulates T-cell signaling, activation, and differentiation [9], and also that GLI2 mediates the transcription of TGF-β1, an immunosuppressive cytokine, during HIV infection [8]. However, it has also been found that Hedgehog signaling, of which GLI2 is an activator, is necessary for wound repair through increased proliferation of fibroblasts and the expression of cytokines [56,57]. As previously reviewed, it seems as though there is a narrow range in which Hedgehog signaling is beneficial for wound repair and T-cell signaling [7]. In the current study, the inhibited expression of GLI2 during persistent VHSV infection at low temperature could be considered as the reason for the failed immune response leading to cell death. Furthermore, the increased expression of GLI2 in the higher temperature virus-infected group could be due to activation of the immune system and hematopoiesis, improving cell survival. In Fig. 3, GLI2 was also shown to be connected to protein tyrosine phosphatase nonreceptor type 6 (PTPN6, a.k.a. SHP-1) through the differentiation of T lymphocytes. In the FHM cell proteomic data, PTPN6 expression was higher at 28 °C than 20 °C, showing that increased response was important in the defense against VHSV. Protein tyrosine phosphatases have been shown to regulate interferon signaling [58], and it has been further shown that PTPN6 plays an important role in the innate immune response to virus infection [59]. In addition, PTPN6 is known to be a key regulator of inflammation in liver hepatocyte-mediated inflammatory response [60]. IPA analysis in Fig. 3 revealed that PTPN6 is also related to inflammation of organ, morbidity or mortality, and cellular homeostasis, making it another possible key biomarker alongside GLI2. In this study, we focused on GLI2 as the central biomarker of VHSV infection.

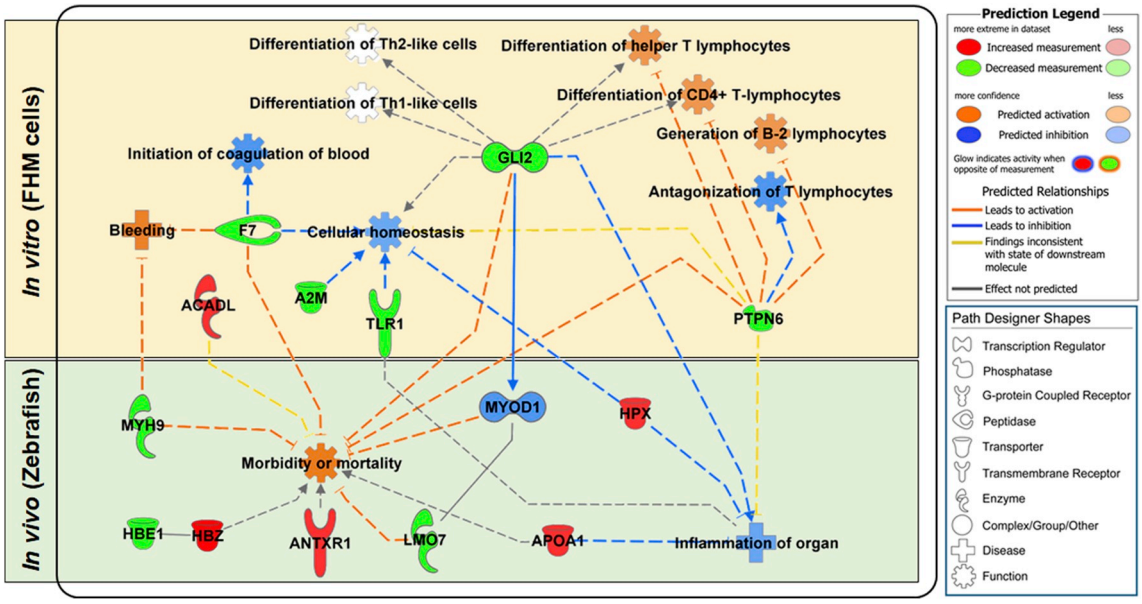


**Fig. 3. Combined network of host response to VHSV infection in FHM cells and zebrafish by IPA.**
Type 1 and Type 2 proteins are represented as virus-infected (V) compared to uninfected (M) at low temperature conditions. FHM cell proteins (20 °C) are shown as 20 V/20M above and zebrafish proteins (15 °C) are shown as 15 V/15M below. Solid lines represent direct connections, dotted lines represent indirect connections.

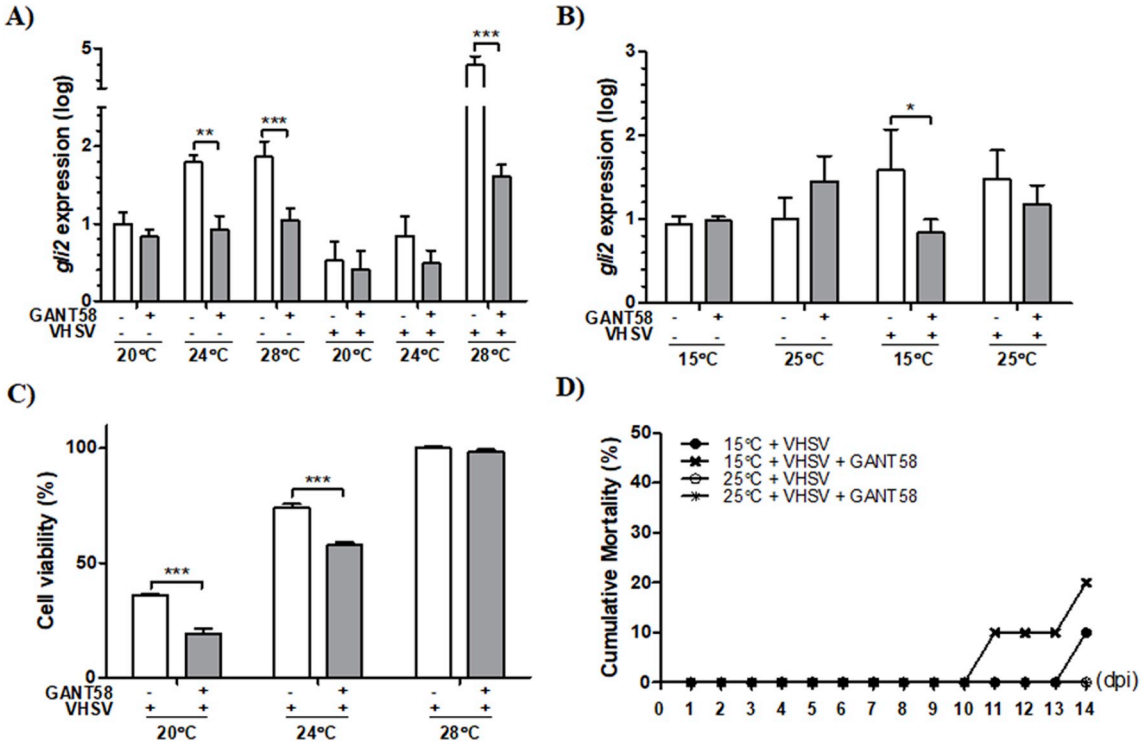


**Fig. 4. Verification of the role of GLI2 in VHSV infection of FHM cells (20 °C to 28 °C) and zebrafish (15 °C and 25 °C) by treatment with GANT58.** GLI2 mRNA expression (A) in FHM cells and (B) in zebrafish. (C) Cell viability of FHM cells and (D) mortality of zebrafish. The concentration of GANT58 used was 100 μM in FHM cells and 100 mg/kg in zebrafish. Error bars represent the mean ± SD (n = 3). *$p \leq 0.05$; **$p \leq 0.01$; ***$p \leq 0.001$ (Bonferroni post-test). VHSV = Viral Hemorrhagic Septicemia virus.

### 3.5. Verification of GLI2 as a regulator of infection

In order to verify the expression of GLI2 in VHSV infection at low and higher temperatures, we inhibited GLI2 activity by treatment with GANT58 [61,62] and investigated the difference in mRNA expression patterns of GLI2 *in vitro* and *in vivo*. In the untreated FHM cells, the expression of GLI2 increased with increasing temperature for both VHSV-infected and uninfected groups (Fig. 4A). GANT58 treatment effectively reduced GLI2 expression in both infected and uninfected cells at all temperatures. While the proteomic analysis showed that the expression was decreased in 28M compared to 20M, GLI2 was increased on the mRNA level. As both samples were collected at 48 hpi, the variation between protein and mRNA expression levels could be high. While mRNA levels are generally reflective of protein levels in a steady state, there is a lag time between transcriptional induction and protein levels in state transitions, which is specific to the organism and to the protein [63]. Both temperature change and virus infections represent a transition state in fish, and this should be taken into consideration. It has also been shown that the protein turnover rate, which can be determined by the half-life of a protein, highly influences the mRNA-protein correlation [64].

In the untreated zebrafish, the mRNA expression of GLI2 showed no significant difference between the different temperatures for both infected and uninfected fish (Fig. 4B). However, the GLI2 expression was significantly increased from the untreated uninfected group to the untreated VHSV-infected group ($p \leq 0.05$). The increase in GLI2 expression in the zebrafish 15 V group may be a temporary increase due to the activation of early immune response at 3 dpi that may not have lasted in later infection stages as discussed above. GANT58 treatment had no significant effect on GLI2 expression at both temperatures during the mock infection. However, it was able to inhibit GLI2 during VHSV infection, especially at 15 °C. Overall, *in vitro* and *in vivo*, the GLI2 expression pattern was shown to be both temperature and virus-dependent in FHM cells, but only virus-dependent in zebrafish, and GANT58 had more efficacy in the cells than in zebrafish. There have been other studies that have shown differences in gene expression *in vitro* and *in vivo*. For example, when comparing the gene expressions of rodent hepatic cells with the whole liver *in vivo*, the cells only showed a weak similarity to the whole liver [65]. In addition, when the *in vitro* and *in vivo* gene expressions in postnatal retinas were compared, there was only a 75% similarity between 8,880 genes from the two systems [66]. In the case of drugs, a study on the effect of viperin against Influenza A virus found viperin to be effective in reducing viral replication *in vitro*, but not *in vivo* when using a viperin-deficient mouse model [67]. Interestingly, while GANT58 was previously shown to protect mice from pulmonary fibrosis through attenuating GLI1, the expression of GLI1 was still higher than the control, which was similar to our results on the effect of GANT58 treatment on GLI2 expression [68].

In terms of cell viability (Fig. 4C), we observed that as GLI2 mRNA expression increased, the cell viability also increased in both GANT58 treated and untreated FHM cells. We also observed that the cell viability decreased due to GANT58 treatment at 20 °C and 24 °C. However, although the cell viability did not decrease at 28 °C, we observed that that treatment of GANT58 at 28 °C significantly increased the VHSV N-gene copy number compared to the untreated cells (Supplementary Fig. S4A). It has been shown by Nishizawa et al. that the viral titer after inoculation and incubation of FHM cells at a high temperature was lower than the titer of the inoculum [69]. They also described that VHSV inoculated at high temperature completely lost its infectivity within two days. Our study also confirmed a reduction in the initial inoculated virus at 28 °C (Supplementary Fig. S4B). This result is encouraging because although the N gene copy number was below the initial number, it was still increased by the inhibition of GLI2 activity. Although the N-gene copy number was increased, it was probably not sufficient for exhibiting a cytopathic effect, so cytopathic effects were not seen in our study. We considered that for this reason, there was no significant difference in cell viability at 28 °C.

In zebrafish, GANT58 treatment caused a faster onset of mortality,

but the total mortality remained the same (Fig. 4D). This was also supported by a 2-log increase in VHSV N gene (Supplementary Fig. S4C). The cumulative mortality of the 15 °C untreated group in Fig. 4D was lower than the mortality in Fig. 1E due to reduced viral replication in the second trial of experiments. Nonetheless, the comparison between untreated and treated VHSV infection at low temperature in zebrafish showed that GANT58 had a significant effect on viral replication, cell viability, and mortality.

While the *in vitro* and *in vivo* models of infection showed conflicting results for the expression of GLI2 without inhibitor treatment, the expressions in both infected models were consistently inhibited by GANT58, and both showed that the expression of GLI2 was stimulated by VHSV infection. Thus, it was shown that GLI2 was one of the main regulators of VHSV infection, alongside other regulators found during the proteomic analysis, that allow for the survival of organisms against VHSV at high temperatures.

## 4. Conclusion

This study revealed that VHSV infection was greatly influenced by modulating the temperature *in vitro* and *in vivo*. The increase in temperature showed a protective effect in both FHM cells and zebrafish. In FHM cells, the higher temperature (28 °C) caused an increase in cell viability and decrease in total apoptosis and VHSV N gene expression; and in zebrafish, the higher temperature (25 °C) caused the disappearance of both the mortality and the detection of the VHSV N gene. The proteome of each infection model was commonly influenced by the modulations of hematological system development and inflammatory response to protect against VHSV infection, and the main protein related to survival in the FHM cell dataset that was also predicted by IPA to be an upstream factor of the zebrafish dataset was GLI2. While it was not found to be the cause for resistance to VHSV at higher temperatures *in vivo*, GLI2 was found to be required for adequate antiviral response *in vitro* and *in vivo*. The controlled regulation of GLI2 or other protein biomarkers revealed through this integrated proteomic analysis can be targeted in the future to create new treatment options against VHSV infection.

## Declarations of interest

None.

## Acknowledgements

This study was supported by a grant from the Korea Basic Science Institute (No. C38711).

## Appendix A. Supplementary data

Supplementary data to this article can be found online at https://doi.org/10.1016/j.fsi.2019.02.037.

## References

[1] C.J.E. Metcalf, K.S. Walter, A. Wesolowski, C.O. Buckee, E. Shevliakova, A.J. Tatem, W.R. Boos, D.M. Weinberger, V.E. Pitzer, Identifying climate drivers of infectious disease dynamics: recent advances and challenges ahead, Proc. R. Soc. B 284 (1860) (2017) 20170901 https://doi.org/10.1098/rspb.2017.0901.

[2] J.E. Linder, K.A. Owers, D.E. Promislow, The effects of temperature on host–pathogen interactions in D. melanogaster: Who benefits? J. Insect Physiol. 54 (1) (2008) 297–308 https://doi.org/10.1016/j.jinsphys.2007.10.001.

[3] A.C. Lowen, S. Mubareka, J. Steel, P. Palese, Influenza virus transmission is dependent on relative humidity and temperature, PLoS Pathog. 3 (10) (2007) e151 https://doi.org/10.1371/journal.ppat.0030151.

[4] T.A. Mace, L. Zhong, C. Kilpatrick, E. Zynda, C.T. Lee, M. Capitano, H. Minderman, E.A. Repasky, Differentiation of CD8+ T cells into effector cells is enhanced by physiological range hyperthermia, J. Leukoc. Biol. 90 (5) (2011) 951–962 https://doi.org/10.1189/jlb.0511229.

[5] E.F. Foxman, J.A. Storer, M.E. Fitzgerald, B.R. Wasik, L. Hou, H. Zhao, P.E. Turner, A.M. Pyle, A. Iwasaki, Temperature-dependent innate defense against the common cold virus limits viral replication at warm temperature in mouse airway cells, Proc. Natl. Acad. Sci. Unit. States Am. 112 (3) (2015) 827–832 https://doi.org/10.1073/pnas.1411030112.

[6] R. Petrova, A.L. Joyner, Roles for Hedgehog signaling in adult organ homeostasis and repair, Development 141 (18) (2014) 3445–3457 https://doi.org/10.1242/dev.083691.

[7] M.G. Smelkinson, The Hedgehog Signaling Pathway Emerges as a Pathogenic Target, J. Dev. Biol. 5 (4) (2017) 14 https://doi.org/10.3390/jdb5040014.

[8] R.L. Furler, C.H. Uittenbogaart, GLI2 regulates TGF-β1 in human CD4+ T cells: implications in cancer and HIV pathogenesis, PLoS One 7 (7) (2012) e40874https://doi.org/10.1371/journal.pone.0040874.

[9] A.L. Furmanski, A. Barbarulo, A. Solanki, C.-I. Lau, H. Sahni, J.I. Saldana, F. D'Acquisto, T. Crompton, The transcriptional activator Gli2 modulates T-cell receptor signalling through attenuation of AP-1 and NFκ-B activity, J. Cell Sci. 128 (11) (2015) 2085–2095 https://doi.org/10.1242/jcs.165803.

[10] H. Colinet, S.F. Lee, A. Hoffmann, Temporal expression of heat shock genes during cold stress and recovery from chill coma in adult Drosophila melanogaster, FEBS J. 277 (1) (2010) 174–185 https://doi.org/10.1111/j.1742-4658.2009.07470.x.

[11] L.R. Pierce, C.A. Stepien, Evolution and biogeography of an emerging quasispecies: diversity patterns of the fish Viral Hemorrhagic Septicemia virus (VHSv), Mol. Phylogenet. Evol. 63 (2) (2012) 327–341 https://doi.org/10.1016/j.ympev.2011.12.024.

[12] Y.S. Kim, C.J. Jang, S.-W. Yeh, Recent surface cooling in the Yellow and East China Seas and the associated North Pacific climate regime shift, Cont. Shelf Res. 156 (2018) 43–54 https://doi.org/10.1016/j.csr.2018.01.009.

[13] A.E. Goodwin, G.E. Merry, Mortality and carrier status of bluegills exposed to viral hemorrhagic septicemia virus genotype IVb at different temperatures, J. Aquat. Anim. Health 23 (2) (2011) 85–91 https://doi.org/10.1080/08997659.2011.574086.

[14] B. Novoa, A. Romero, V. Mulero, I. Rodríguez, I. Fernández, A. Figueras, Zebrafish (Danio rerio) as a model for the study of vaccination against viral haemorrhagic septicemia virus (VHSV), Vaccine 24 (31–32) (2006) 5806–5816 https://doi.org/10.1016/j.vaccine.2006.05.015.

[15] K. Muroga, Viral and bacterial diseases of marine fish and shellfish in Japanese hatcheries, Aquaculture 202 (1–2) (2001) 23–44 https://doi.org/10.1016/S0044-8486(01)00597-X.

[16] M.K. Purcell, K.J. Laing, J.R. Winton, Immunity to fish rhabdoviruses, Viruses 4 (1) (2012) 140–166 https://doi.org/10.1016/S0044-8486(01)00597-X.

[17] P. Dixon, R. Paley, R. Alegria-Moran, B. Oidtmann, Epidemiological characteristics of infectious hematopoietic necrosis virus (IHNV): a review, Vet. Res. 47 (1) (2016) 63 https://doi.org/10.1186/s13567-016-0341-1.

[18] P. Jiravanichpaisal, K. Söderhäll, I. Söderhäll, Effect of water temperature on the immune response and infectivity pattern of white spot syndrome virus (WSSV) in freshwater crayfish, Fish Shellfish Immunol. 17 (3) (2004) 265–275 https://doi.org/10.1016/j.fsi.2004.03.010.

[19] R. Kim, M. Faisal, Emergence and resurgence of the viral hemorrhagic septicemia virus (Novirhabdovirus, Rhabdoviridae, Mononegavirales), J. Adv. Res. 2 (1) (2011) 9–23 https://doi.org/10.1016/j.jare.2010.05.007.

[20] N. Vo, A. Bender, L. Lee, J. Lumsden, N. Lorenzen, B. Dixon, N. Bols, Development of a walleye cell line and use to study the effects of temperature on infection by viral haemorrhagic septicaemia virus group IV b, J. Fish. Dis. 38 (2) (2015) 121–136 https://doi.org/10.1111/jfd.12208.

[21] P. Hershberger, M. Purcell, L. Hart, J. Gregg, R. Thompson, K. Garver, J. Winton, Influence of temperature on viral hemorrhagic septicemia (Genogroup IVa) in Pacific herring, Clupea pallasii Valenciennes, J. Exp. Mar. Biol. Ecol. 444 (2013) 81–86 https://doi.org/10.1016/j.jembe.2013.03.006.

[22] T. Isshiki, T. Nagano, T. Miyazaki, Effect of water temperature on pathological states of Japanese flounder [Paralichthys olivaceus] experimentally infected with viral hemorrhagic septicemia virus, an flounder isolate KRRV-9601, Fish Pathol. 37 (2) (2002) 95–97 https://doi.org/10.3147/jsfp.37.95.

[23] T. Isshiki, T. Nishizawa, T. Kobayashi, T. Nagano, T. Miyazaki, An outbreak of VHSV (viral hemorrhagic septicemia virus) infection in farmed Japanese flounder Paralichthys olivaceus in Japan, Dis. Aquat. Org. 47 (2) (2001) 87–99 https://doi.org/10.3354/dao047087.

[24] K.-i. Mori, H. Iida, T. Nishizawa, M. Arimoto, K. Nakajima, K. Muroga, Properties of viral hemorrhagic septicemia virus (VHSV) isolated from Japanese flounder Paralichthys olivaceus, Fish Pathol. 37 (4) (2002) 169–174 https://doi.org/10.3147/jsfp.37.169.

[25] C. Tafalla, J. Coll, C. Secombes, Expression of genes related to the early immune response in rainbow trout (Oncorhynchus mykiss) after viral haemorrhagic septicemia virus (VHSV) infection, Dev. Comp. Immunol. 29 (7) (2005) 615–626 https://doi.org/10.1016/j.dci.2004.12.001.

[26] S.-J. Kim, J.-O. Kim, W.-S. Kim, M.-J. Oh, Viral hemorrhagic septicemia virus (VHSV) infectivity dynamics in olive flounder, Paralichthys olivaceus with injection and immersion challenge routes, Aquaculture 465 (2016) 7–12 https://doi.org/10.1016/j.aquaculture.2016.08.025.

[27] S.-Y. Cho, J. Kwon, B. Vaidya, J.-O. Kim, S. Lee, E.-H. Jeong, K.S. Baik, J.-S. Choi, H.-J. Bae, M.-J. Oh, Modulation of proteome expression by F-type lectin during viral hemorrhagic septicemia virus infection in fathead minnow cells, Fish Shellfish Immunol. 39 (2) (2014) 464–474 https://doi.org/10.1016/j.fsi.2014.05.042.

[28] E.-H. Jeong, B. Vaidya, S.-Y. Cho, M.-A. Park, K. Kaewintajuk, S.R. Kim, M.-J. Oh, J.-S. Choi, J. Kwon, D. Kim, Identification of regulators of the early stage of viral hemorrhagic septicemia virus infection during curcumin treatment, Fish Shellfish Immunol. 45 (1) (2015) 184–193 https://doi.org/10.1016/j.fsi.2015.03.042.

[29] P. Encinas, M.A. Rodriguez-Milla, B. Novoa, A. Estepa, A. Figueras, J. Coll,

Zebrafish fin immune responses during high mortality infections with viral haemorrhagic septicemia rhabdovirus. A proteomic and transcriptomic approach, BMC Genomics 11 (1) (2010) 518 https://doi.org/10.1186/1471-2164-11-518.
[30] M. Dang, R.E. Henderson, L.A. Garraway, L.I. Zon, Long-term drug administration in the adult zebrafish using oral gavage for cancer preclinical studies, Dis. Models Mech. 9 (2016) 811–820 https://doi.org/10.1242/dmm.024166.
[31] P. Kulkarni, G.H. Chaudhari, V. Sripuram, R.K. Banote, K. T Kirla, R. Sultana, P. Rao, S. Oruganti, K. Chatti, Oral dosing in adult zebrafish: proof-of-concept using pharmacokinetics and pharmacological evaluation of carbamazepine, Pharmacol. Rep. 66 (1) (2014) 179–183 https://doi.org/10.1016/j.pharep.2013.06.012.
[32] L.J. Reed, H. Muench, A simple method of estimating fifty per cent endpoints, Am. J. Epidemiol. 27 (3) (1938) 493–497 https://doi.org/10.1093/oxfordjournals.aje.a118408.
[33] C.-L. Han, C.-W. Chien, W.-C. Chen, Y.-R. Chen, C.-P. Wu, H. Li, Y.-J. Chen, A multiplexed quantitative strategy for membrane proteomics opportunities for mining therapeutic targets for autosomal dominant polycystic kidney disease, Mol. Cell. Proteomics 7 (10) (2008) 1983–1997 https://doi.org/10.1074/mcp.M800068-MCP200.
[34] H.-Y. Yang, J. Kwon, E.-J. Cho, H.-I. Choi, C. Park, H.-R. Park, S.-H. Park, K.-J. Chung, Z.Y. Ryoo, K.-O. Cho, Proteomic analysis of protein expression affected by peroxiredoxin V knock-down in hypoxic kidney, J. Proteome Res. 9 (8) (2010) 4003–4015 https://doi.org/10.1021/pr100190b.
[35] J.G. Burniston, J. Connolly, H. Kainulainen, S.L. Britton, L.G. Koch, Label-free profiling of skeletal muscle using high-definition mass spectrometry, Proteomics 14 (20) (2014) 2339–2344 https://doi.org/10.1002/pmic.201400118.
[36] J.-O. Kim, W.-S. Kim, S.-W. Kim, H.-J. Han, J.W. Kim, M. Park, M.-J. Oh, Development and application of quantitative detection method for viral hemorrhagic septicemia virus (VHSV) genogroup IVa, Viruses 6 (5) (2014) 2204–2213 https://doi.org/10.3390/v6052204.
[37] H.R. Jayakar, E. Jeetendra, M.A. Whitt, Rhabdovirus assembly and budding, Virus Res. 106 (2) (2004) 117–132 https://doi.org/10.1016/j.virusres.2004.08.009.
[38] C. Sullivan, C.H. Kim, Zebrafish as a model for infectious disease and immune function, Fish Shellfish Immunol. 25 (4) (2008) 341–350 https://doi.org/10.1016/j.fsi.2008.05.005.
[39] S.-Y. Cho, Y.-K. Kwon, M. Nam, B. Vaidya, S.R. Kim, S. Lee, J. Kwon, D. Kim, G.-S. Hwang, Integrated profiling of global metabolomic and transcriptomic responses to viral hemorrhagic septicemia virus infection in olive flounder, Fish Shellfish Immunol. 71 (2017) 220–229 https://doi.org/10.1016/j.fsi.2017.10.007.
[40] W.-S. Kim, S.-R. Kim, D. Kim, J.-O. Kim, M.-A. Park, S.-I. Kitamura, H.-Y. Kim, D.-H. Kim, H.-J. Han, S.-J. Jung, An outbreak of VHSV (viral hemorrhagic septicemia virus) infection in farmed olive flounder Paralichthys olivaceus in Korea, Aquaculture 296 (1–2) (2009) 165–168 https://doi.org/10.1016/j.aquaculture.2009.07.019.
[41] S. Avunje, M.-J. Oh, S.-J. Jung, Impaired TLR2 and TLR7 response in olive flounder infected with viral haemorrhagic septicaemia virus at host susceptible 15 C but high at non-susceptible 20 C, Fish Shellfish Immunol. 34 (5) (2013) 1236–1243 https://doi.org/10.1016/j.fsi.2013.02.012.
[42] R. Castro, B. Abós, J. Pignatelli, L. von Gersdorff Jørgensen, A.G. Granja, K. Buchmann, C. Tafalla, Early immune responses in rainbow trout liver upon viral hemorrhagic septicemia virus (VHSV) infection, PLoS One 9 (10) (2014) e111084https://doi.org/10.1371/journal.pone.0111084.
[43] S. Avunje, W.-S. Kim, M.-J. Oh, I. Choi, S.-J. Jung, Temperature-dependent viral replication and antiviral apoptotic response in viral haemorrhagic septicaemia virus (VHSV)-infected olive flounder (Paralichthys olivaceus), Fish Shellfish Immunol. 32 (6) (2012) 1162–1170 https://doi.org/10.1016/j.fsi.2012.03.025.
[44] J.Y. Hwang, K. Markkandan, K. Han, M.G. Kwon, J.S. Seo, S.-i. Yoo, S.D. Hwang, B.Y. Ji, M.-H. Son, J.-h. Park, Temperature-dependent immune response of olive flounder (Paralichthys olivaceus) infected with viral hemorrhagic septicemia virus (VHSV), Gene Genom. 40 (3) (2018) 315–320 https://doi.org/10.1007/s13258-017-0638-0.
[45] F. Nainu, A. Shiratsuchi, Y. Nakanishi, Induction of apoptosis and subsequent phagocytosis of virus-infected cells as an antiviral mechanism, Front. Immunol. 8 (2017) 1220 https://doi.org/10.3389/fimmu.2017.01220.
[46] C.A. Janeway Jr., P. Travers, M. Walport, M.J. Shlomchik, The components of the immune system, Immunobiology: The Immune System in Health and Disease, fifth ed., Garland Science, New York, 2001.
[47] P. Pereiro, S. Dios, S. Boltaña, J. Coll, A. Estepa, S. Mackenzie, B. Novoa, A. Figueras, Transcriptome profiles associated to VHSV infection or DNA vaccination in turbot (Scophthalmus maximus), PLoS One 9 (8) (2014) e104509https://doi.org/10.1371/journal.pone.0104509.
[48] S. Antoniak, N. Mackman, Multiple roles of the coagulation protease cascade during virus infection, Blood 123 (17) (2014) 2605–2613 https://doi.org/10.1182/blood-2013-09-526277.
[49] N.S. Key, G.M. Vercellotti, J.C. Winkelmann, C.F. Moldow, J.L. Goodman, N.L. Esmon, C.T. Esmon, H.S. Jacob, Infection of vascular endothelial cells with herpes simplex virus enhances tissue factor activity and reduces thrombomodulin expression, Proc. Natl. Acad. Sci. Unit. States Am. 87 (18) (1990) 7095–7099.
[50] T.W. Geisbert, H.A. Young, P.B. Jahrling, K.J. Davis, E. Kagan, L.E. Hensley, Mechanisms underlying coagulation abnormalities in ebola hemorrhagic fever: overexpression of tissue factor in primate monocytes/macrophages is a key event, J. Infect. Dis. 188 (11) (2003) 1618–1629 https://doi.org/10.1086/379724.
[51] A. Huerta-Zepeda, C. Cabello-Gutiérrez, J. Cime-Castillo, V. Monroy-Martínez, M.E. Manjarrez-Zavala, M. Gutiérrez-Rodríguez, R. Izaguirre, B.H. Ruiz-Ordaz, Crosstalk between coagulation and inflammation during Dengue virus infection, Thromb. Haemostasis 100 (05) (2008) 936–943 https://doi.org/10.1160/TH07-08-0483.
[52] N.T. Funderburg, E. Mayne, S.F. Sieg, R. Asaad, W. Jiang, M. Kalinowska, A.A. Luciano, W. Stevens, B. Rodriguez, J.M. Brenchley, Increased tissue factor expression on circulating monocytes in chronic HIV infection: relationship to in vivo coagulation and immune activation, Blood 115 (2) (2010) 161–167 https://doi.org/10.1182/blood-2009-03-210179.
[53] L.C. Petersen, E. Persson, P.O. Freskgård, Thermal effects on an enzymatically latent conformation of coagulation factor VIIa, Eur. J. Biochem. 261 (1) (1999) 124–129 https://doi.org/10.1046/j.1432-1327.1999.00258.x.
[54] A. Voronova, E. Coyne, A. Al Madhoun, J.V. Fair, N. Bosiljcic, C. St-Louis, G. Li, S. Thurig, V.A. Wallace, N. Wiper-Bergeron, Hedgehog signaling regulates MyoD expression and activity, J. Biol. Chem. 288 (6) (2013) 4389–4404 https://doi.org/10.1074/jbc.M112.400184.
[55] C.L. Himeda, M.V. Barro, C.P. Emerson Jr., Pax3 synergizes with Gli2 and Zic1 in transactivating the Myf5 epaxial somite enhancer, Dev. Biol. 383 (1) (2013) 7–14 https://doi.org/10.1016/j.ydbio.2013.09.006.
[56] J. Asai, H. Takenaka, K.F. Kusano, M. Ii, C. Luedemann, C. Curry, E. Eaton, A. Iwakura, Y. Tsutsumi, H. Hamada, Topical sonic hedgehog gene therapy accelerates wound healing in diabetes by enhancing endothelial progenitor cell–mediated microvascular remodeling, Circulation 113 (20) (2006) 2413–2424 https://doi.org/10.1161/CIRCULATIONAHA.105.603167.
[57] E. Mathew, M.A. Collins, M.G. Fernandez-Barrena, A.M. Holtz, W. Yan, J.O. Hogan, Z. Tata, B.L. Allen, M.E. Fernandez-Zapico, M.P. Di Magliano, The transcription factor GLI1 modulates the inflammatory response during pancreatic tissue remodeling, J. Biol. Chem. 289 (40) (2014) 27727–27743 https://doi.org/10.1074/jbc.M114.556563.
[58] W.J. Stanley, S.A. Litwak, H.S. Quah, S.M. Tan, T.W.H. Kay, T. Tiganis, J.B. de Haan, H.E. Thomas, E.N. Gurzov, Inactivation of protein tyrosine phosphatases enhances interferon signaling in pancreatic islets, Diseases 64 (2015) 2489–2496 https://doi.org/10.2337/db14-1575.
[59] K.L. Bonaparte, C.A. Hudson, C. Wu, P.T. Massa, Inverse regulation of inducible nitric oxide synthase (iNOS) and arginase I by the protein tyrosine phosphatase SHP-1 in CNS glia, Glia 53 (8) (2006) 827–835 https://doi.org/10.1002/glia.20344.
[60] A. Adhikari, C. Martel, A. Marette, M. Olivier, Hepatocyte SHP-1 is a key modulator of inflammation during endotoxemia, Sci. Rep. 7 (2017) 2218 https://doi.org/10.1038/s41598-017-02512-7.
[61] X. Hou, X. Chen, P. Zhang, Y. Fan, A. Ma, T. Pang, Z. Song, Y. Jin, W. Hao, F. Liu, Inhibition of hedgehog signaling by GANT58 induces apoptosis and shows synergistic antitumor activity with AKT inhibitor in acute T cell leukemia cells, Biochimie 101 (2014) 50–59 https://doi.org/10.1016/j.biochi.2013.12.019.
[62] M. Lauth, Å. Bergström, T. Shimokawa, R. Toftgård, Inhibition of GLI-mediated transcription and tumor cell growth by small-molecule antagonists, Proc. Natl. Acad. Sci. Unit. States Am. 104 (20) (2007) 8455–8460 https://doi.org/10.1073/pnas.0609699104.
[63] Y. Liu, A. Beyer, R. Aebersold, On the dependency of cellular protein levels on mRNA abundance, Cell 165 (3) (2016) 535–550 https://doi.org/10.1016/j.cell.2016.03.014.
[64] T. Maier, M. Güell, L. Serrano, Correlation of mRNA and protein in complex biological samples, FEBS Lett. 583 (24) (2009) 3966–3973 https://doi.org/10.1016/j.febslet.2009.10.036.
[65] F. Boess, M. Kamber, S. Romer, R. Gasser, D. Muller, S. Albertini, L. Suter, Gene expression in two hepatic cell lines, cultured primary hepatocytes, and liver slices compared to the in vivo liver gene expression in rats: possible implications for toxicogenomics use of in vitro systems, Toxicol. Sci. 73 (2) (2003) 386–402 https://doi.org/10.1093/toxsci/kfg064.
[66] M.-G. Liu, H. Li, X. Xu, C.J. Barnstable, S.S.-M. Zhang, Comparison of gene expression during in vivo and in vitro postnatal retina development, J. Ocular Biol., Dis. Inf. 1 (2–4) (2008) 59–72 https://doi.org/10.1007/s12177-008-9009-z.
[67] K.S. Tan, F. Olfat, M.C. Phoon, J.P. Hsu, J.L. Howe, J.E. Seet, K.C. Chin, V.T. Chow, In vivo and in vitro studies on the antiviral activities of viperin against influenza H1N1 virus infection, J. Gen. Virol. 93 (6) (2012) 1269–1277 https://doi.org/10.1099/vir.0.040824-0.
[68] X. Chen, C. Shi, H. Cao, L. Chen, J. Hou, Z. Xiang, K. Hu, X. Han, The hedgehog and Wnt/β-catenin system machinery mediate myofibroblast differentiation of LR-MSCs in pulmonary fibrogenesis, Cell Death Dis. 9 (6) (2018) 639 https://doi.org/10.1038/s41419-018-0692-9.
[69] T. Nishizawa, I. Takami, M. Yang, M.-J. Oh, Live vaccine of viral hemorrhagic septicemia virus (VHSV) for Japanese flounder at fish rearing temperature of 21 °C instead of Poly(I:C) administration, Vaccine 29 (2011) 8397–8404 https://doi.org/10.1016/j.vaccine.2011.08.032.